AMERICAN SOCIETY FOR MICROBIOLOGY | Molecular and Cellular Biology®

RESEARCH ARTICLE

Phosphorylation of Translation Initiation Factor 2-Alpha in *Leishmania donovani* under Stress Is Necessary for Parasite Survival

Kumar Abhishek,[a] Abul Hasan Sardar,[a] Sushmita Das,[b] Ashish Kumar,[a] Ayan Kumar Ghosh,[a] Ruby Singh,[a] Savita Saini,[c] Abhishek Mandal,[a] Sudha Verma,[a] Ajay Kumar,[a] Bidyut Purkait,[a] Manas Ranjan Dikhit,[d] Pradeep Das[a]

Division of Molecular Biology, Rajendra Memorial Research Institute of Medical Sciences, Agamkuan, Patna, Bihar, India[a]; Department of Microbiology, All India Institute of Medical Sciences, Phulwarisharif, Patna, Bihar, India[b]; National Institute of Pharmaceutical Education and Research, Export Promotion Industrial Park, Hajipur, Vaishali, Bihar, India[c]; Department of Bioinformatics, Rajendra Memorial Research Institute of Medical Sciences, Agamkuan, Patna, Bihar, India[d]

ABSTRACT The transformation of *Leishmania donovani* from a promastigote to an amastigote during mammalian host infection displays the immense adaptability of the parasite to survival under stress. Induction of translation initiation factor 2-alpha (eIF2α) phosphorylation by stress-specific eIF2α kinases is the basic stress-perceiving signal in eukaryotes to counter stress. Here, we demonstrate that elevated temperature and acidic pH induce the phosphorylation of *Leishmania donovani* eIF2α (LdeIF2α). *In vitro* inhibition experiments suggest that interference of LdeIF2α phosphorylation under conditions of elevated temperature and acidic pH debilitates parasite differentiation and reduces parasite viability ($P < 0.05$). Furthermore, inhibition of LdeIF2α phosphorylation significantly reduced the infection rate ($P < 0.05$), emphasizing its deciding role in successful invasion and infection establishment. Notably, our findings suggested the phosphorylation of LdeIF2α under H_2O_2-induced oxidative stress. Inhibition of H_2O_2-induced LdeIF2α phosphorylation hampered antioxidant balance by impaired redox homeostasis gene expression, resulting in increased reactive oxygen species accumulation ($P < 0.05$) and finally leading to decreased parasite viability ($P < 0.05$). Interestingly, exposure to sodium antimony glucamate and amphotericin B induces LdeIF2α phosphorylation, indicating its possible contribution to protection against antileishmanial drugs in common use. Overall, the results strongly suggest that stress-induced LdeIF2α phosphorylation is a necessary event for the parasite life cycle under stressed conditions for survival.

KEYWORDS LdeIF2α phosphorylation, pH stress, temperature stress, oxidative stress, GSK2606414, *Leishmania* survival

Received 14 June 2016 **Returned for modification** 3 July 2016 **Accepted** 13 September 2016

Accepted manuscript posted online 10 October 2016

Citation Abhishek K, Sardar AH, Das S, Kumar A, Ghosh AK, Singh R, Saini S, Mandal A, Verma S, Kumar A, Purkait B, Dikhit MR, Das P. 2017. Phosphorylation of translation initiation factor 2-alpha in *Leishmania donovani* under stress is necessary for parasite survival. Mol Cell Biol 37:e00344-16. https://doi.org/10.1128/MCB.00344-16.

Address correspondence to Pradeep Das, drpradeep.das@gmail.com.

Leishmaniasis is caused by various species of *Leishmania*, a protozoan parasite which alternates between a flagellar, motile promastigote form in sand fly and an aflagellar, nonmotile amastigote form in mammalian hosts preceding successful invasion. Stress-induced transformation inside mammalian macrophages adapts the parasite to thrive in the harsh phagolysosomal environment, achieved by modulating gene expression at both the transcriptional and posttranscriptional levels (1–4).

Reversible phosphorylation of the α-subunit of eukaryotic translation initiation factor 2-alpha (eIF2α) at serine 51 by stress-responsive kinases is a basic posttranscriptional event, affecting the global protein synthesis rate while promoting the cell synthesis of stress-responsive genes (5–7).

The phosphorylation of eIF2α under stress conditions is a major survival response that is conserved from yeast to mammals and plays a significant role when cells must respond to environmental stresses. In protozoan parasites, eIF2α phosphorylation may be induced under different cytoplasmic stresses such as elevated temperature, acidic pH, and nutritional stress and oxidative stress generated by arsenite treatment. Stress-induced phosphorylation of eIF2α plays a crucial role in the life cycle events of protozoan parasites, mediates differentiation, and maintains the latent form required for the parasite to adapt to and survive in the stressed environment inside the host. In *Toxoplasma gondii*, TgeIF2α phosphorylation is important for maintaining the latency of the bradyzoite form in the mammalian host (8). Moreover, it has been reported that phosphorylation of eIF2α in *Toxoplasma gondii* is critical for the resistance of the parasite to external stress outside its host; inhibition of this phosphorylation significantly delays the development of acute toxoplasmosis *in vivo* (9). In *Plasmodium*, phosphorylation of PfeIF2α is essential for the development of the erythrocytic cycle (10), and nutritional stress-induced eIF2α phosphorylation in *Trypanosoma cruzi* regulates metacyclogenesis (11). In *Leishmania infantum*, phosphorylation of eIF2α has been interpreted with the differentiation of the parasite under concomitant exposure to high temperature and acidic pH (12).

Phosphorylation of eIF2α is mediated by different eIF2α kinases that respond to specific environmental stresses, facilitating programs of stress-induced gene expression. The eIF2α kinases are a family of four well-characterized serine-threonine kinases: PERK (PKR-like endoplasmic reticulum [ER] kinase) responds to protein misfolding in the endoplasmic reticulum, PKR (double-stranded RNA-dependent protein kinase) plays a key role in the cellular antiviral response, GCN2 (general control nonderepressible 2) is activated during amino acid starvation, and HRI (heme-regulated inhibitor) limits protein synthesis during heme deficiency (13).

Knowledge regarding protozoan eIF2α kinases is in its initial stage. In *Plasmodium*, three eIF2α serine-threonine kinases, eIK1, eIK2, and PK4, have been identified with stage-specific expression (14), of which PK4 mediates translational repression in schizonts and is essential for the erythrocytic cycle in *Plasmodium falciparum* (10). *Toxoplasma brucei* TbeIF2K1 and TbeIF2K2, the first one of which is of the GCN2 type (15), and *Toxoplasma gondii* PERK-type TgIF2K-A and TgIF2K-B kinases have been reported in relation to the development of latent cysts under stress (8). However, eIF2α kinases in protozoan parasites are regulated mostly by changes in physiological parameters such as temperature and pH, although recently, a different type of eIF2α kinase in *Trypanosoma cruzi* was reported, which is regulated by heme deficiency and which controls differentiation and reactive oxygen species (ROS) levels (16). For *Leishmania* species, very little information is available, concentrated mainly on PERK (17, 18).

In higher eukaryotes, stress-induced phosphorylation of eIF2α is associated with many diseases and is involved in metabolic pathways such as apoptosis, autophagy, maintenance of intracellular antioxidant levels, and protection against oxidative stress (19). In humans, eIF2α is a critical regulatory factor in the response of nerve cells to oxidative stress and in the control of the level of the major intracellular antioxidant glutathione (GSH) and plays a central role in the many neurodegenerative diseases associated with protection against oxidative stress (20, 21).

Here, we report that elevated temperature and acidic pH, physiological conditions prevailing inside the phagolysosomal compartment or conditions triggering promastigote-to-amastigote transformation, induce *L. donovani* eIF2α (LdeIF2α) phosphorylation. Apart from this, oxidative stress generated by H_2O_2 or the practiced antileishmanial drugs sodium antimony glucamate (SAG) and amphotericin B (Amp B) also serves as a potent inducer of LdeIF2α phosphorylation. We used GSK2606414 (GSK), a PERK inhibitor, and found that it inhibits the phosphorylation of LdeIF2α under stress conditions (22). *In vitro* experiments showed that the inhibition of LdeIF2α phosphorylation under conditions of H_2O_2 exposure reduces the total antioxidant level, decreases the expression levels of redox homeostasis genes, tends to accumulate ROS, and consequently leads to a significant decrease in parasite viability. There is also a possibility of an involvement in protection against drug-

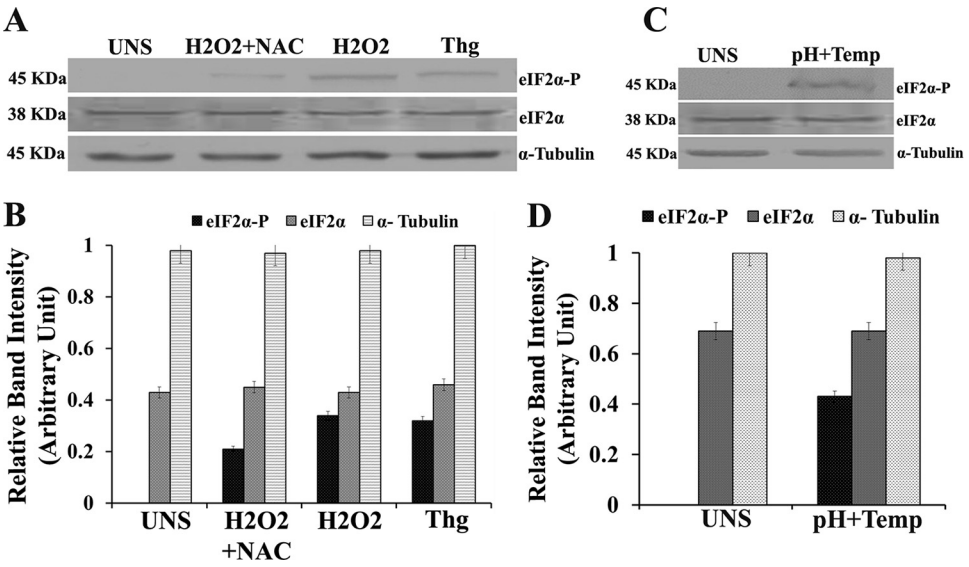

FIG 1 *Leishmania donovani* translation initiation factor 2-alpha (LdeIF2α) is phosphorylated under stress conditions. (A) *L. donovani* promastigotes exposed to H_2O_2 (200 μM), NAC plus H_2O_2 stress, and thapsigargin (Thg) (1 μM) for 4 h. Untreated promastigotes (UNS) served as a control. (B) Densitometry of Western blot bands. (C) *L. donovani* promastigotes exposed to a combination of high-temperature and low-pH (pH 5.5) stress for 4 h. The cells were lysed, and the whole-cell lysates were immunoreacted with a rabbit polyclonal anti-eIF2α (pS51)-phosphospecific antibody (eIF2α-P) to detect eIF2α phosphorylation. (D) Relative band intensities of lanes. Protein loading was monitored by using an anti-*Leishmania*-specific eIF2α antibody and an anti-α-tubulin antibody.

induced stress. Under conditions of elevated temperature and acidic pH, LdeIF2α phosphorylation impairment delays the differentiation process, leading to decreased parasite viability. Similarly, an infection study in mouse peritoneal exudate cells (PECs) also showed decreased infection by GSK2606414-treated parasites, indicating the crucial role of LdeIF2α phosphorylation under stress for the establishment of infection. Taken together, these findings indicate that stress-induced phosphorylation of LdeIF2α plays a crucial role in differentiation and parasite survival under stress.

RESULTS

***Leishmania donovani* translation initiation factor 2-alpha is phosphorylated under stress.** To determine the phosphorylation status of LdeIF2α under stress conditions, Western blot analysis using a phosphospecific antibody against eIF2α was carried out after treatment of parasites with thapsigargin (Thg), an ER stress generator, and the ROS inducer H_2O_2 for 4 h in the presence or absence of the ROS scavenger *N*-acetyl cysteine (NAC). As shown in Fig. 1, LdeIF2α was found to be phosphorylated in promastigotes exposed to H_2O_2, but in cases of parasites treated with NAC (H_2O_2 plus NAC), a comparatively low level of LdeIF2α phosphorylation was detected (Fig. 1A). No phosphorylation was detected in the case of control unstressed (UNS) parasites. LdeIF2α phosphorylation was also detected in promastigotes treated with Thg. Densitometric analysis of Western blots indicated that the level of phosphorylation of LdeIF2α was ~2-fold higher in H_2O_2-treated parasites than in parasites incubated with H_2O_2 plus NAC (Fig. 1B). Similarly, LdeIF2α phosphorylation was also observed (Fig. 1C) when *L. donovani* promastigotes were exposed to a combination of high temperature (37°C) and low pH (pH 5.5) for 4 h, conditions known to trigger the conversion of promastigotes to the pathogenic amastigote form. These results clearly suggest that elevated temperature/acidic pH (37°C/pH 5.5) and H_2O_2 induce LdeIF2α phosphorylation in *L. donovani* promastigotes.

SAG and amphotericin B also induce LdeIF2α phosphorylation. Common antileishmanial drugs such as SAG and Amp B also act on the parasite through ROS generation. To further explore the effect of these drugs on the phosphorylation status of LdeIF2α, *L. donovani* promastigotes were exposed to two concentrations of SAG (40

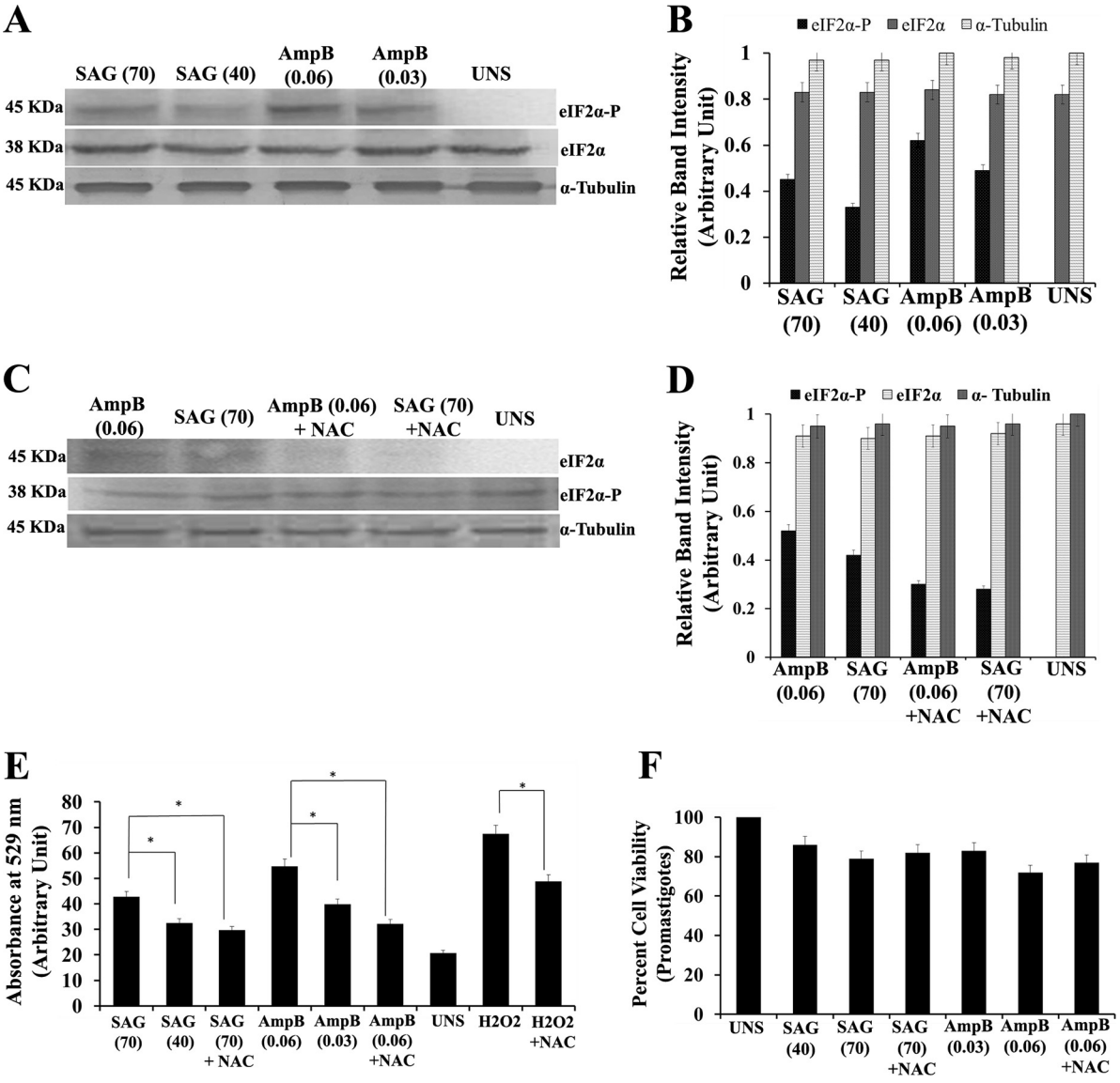

FIG 2 SAG and amphotericin B also induce LdeIF2α phosphorylation. (A) Western blotting to determine the phosphorylation status of LdeIF2α upon exposure to the antileishmanial drugs sodium antimony glucamate (SAG) and amphotericin B (Amp B). *L. donovani* promastigotes were exposed two different doses, *viz.*, SAG_{40} and SAG_{70} for SAG and Amp $B_{0.06}$ and Amp $B_{0.03}$ for Amp B for 8 h and immunoreacted with rabbit polyclonal anti-eIF2α (pS51)-phosphospecific antibody. Parasites without any stress served as controls (UNS). Protein loading was monitored by using an anti-*Leishmania*-specific eIF2α antibody and an anti-α-tubulin antibody. (B) Relative phosphorylation status determined by densitometry. (C) Western blotting to determine LdeIF2α phosphorylation upon exposure to SAG_{70}, SAG plus NAC, Amp $B_{0.06}$, or Amp B plus NAC after 8 h of treatment. (D) Densitometric analysis of band intensities. (E) ROS generation determined spectrofluorimetrically by using H_2DCFDA dye under the above-mentioned conditions. *L. donovani* promastigotes exposed to H_2O_2 (200 μM) served as positive controls for ROS measurement. (F) Percent viability of promastigotes exposed to SAG_{40}, SAG_{70}, SAG_{70} plus NAC, Amp $B_{0.03}$, Amp $B_{0.06}$, or Amp $B_{0.06}$ plus NAC. UNS parasites were used as controls. Values are the means and SDs of results from three independent experiments. (Significant differences are indicated by * [$P < 0.05$].)

μM and 70 μM) and Amp B (0.030 μM and 0.060 μM) for 8 h. Western blot analysis showed that LdeIF2α was phosphorylated at both doses of SAG and Amp B (Fig. 2A). Densitometric analysis of Western blots showed a lower level of phosphorylation with SAG than with Amp B exposure (Fig. 2B). To further ensure that drug-generated ROS induce LdeIF2α phosphorylation, NAC treatment along with SAG (70 μM) or Amp B (0.060 μM) treatment was performed (Fig. 2C). A low level of phosphorylation was found, as revealed by densitometry analysis of bands (Fig. 2D). Thus, this result suggests that both SAG and amphotericin B also induce LdeIF2α phosphorylation. It was previously reported that the mode of action of SAG and amphotericin B includes ROS

generation to clear parasite infection. We analyzed intracellular ROS generation in promastigotes using 2′,7′-dichlorodihydrofluorescein diacetate (H_2DCFDA) dye. The ROS level for *L. donovani* promastigotes exposed to the higher dose of 70 μM SAG (SAG_{70}) was found to be ~1.2-fold higher ($P < 0.05$) than that for promastigotes exposed to the lower dose (SAG_{40}). Similarly, for amphotericin B treatment, promastigotes subjected to the higher dose of Amp B (Amp $B_{0.06}$) showed ~1.3-fold-higher ($P < 0.05$) ROS accumulation than did promastigotes subjected to the lower dose of Amp B (Amp $B_{0.03}$). Again, parasites incubated with NAC and subjected to drug exposure showed a low level of ROS accumulation compared to that without NAC (Fig. 2E). Thus, the association observed between the ROS level and the level of LdeIF2α phosphorylation, independent of the dose and drug used, indicates the role of ROS in mediating LdeIF2α phosphorylation. Cell viabilities 8 h after drug treatment, as estimated by 3-(4,5-dimethyl-2-thiazolyl)-2,5-diphenyl-2H-tetrazolium bromide (MTT) assays, were found to be 89% and 82% at 40 μM and 70 μM SAG, respectively, and 82% and 78% at 0.03 μM and 0.06 μM Amp B, respectively, compared to untreated parasites. For parasites incubated with NAC and subjected to drug treatment, higher cell viability was recorded (Fig. 2F). Importantly, the observed differences in cell viability were found to be insignificant.

LdeIF2α phosphorylation during promastigote-to-amastigote transformation decreases global translation. Studies of protein synthesis frequently utilize polyribosome or polysome (mRNA/ribosome complex) analysis to shed light on the defects in protein synthesis in eukaryotic cells, including *Leishmania* (12, 18). A sucrose density gradient separates mRNAs bound to multiple ribosomes, which are further analyzed by determining the optical density (OD) at 254 nm to obtain a polysome profile. To observe the global translational level of parasites during differentiation, polysome profile analysis was carried out by using *L. donovani* promastigotes and axenic amastigotes. First, promastigotes were converted to axenic amastigotes according to the protocols described in Materials and Methods and were examined microscopically after 4 days of treatment. Elongated and flagellated promastigotes were converted to rounded and nonflagellated amastigote-like form (Fig. 3A). The polysome profile was found to be significantly decreased in axenic amastigotes demonstrating a low global translation rate compared to that of promastigotes (Fig. 3B). Simultaneously, LdeIF2α phosphorylation was detected in axenic amastigotes by Western blotting using anti-phosphospecific eIF2α antibody (pS51); however, no such phosphorylation was detected in promastigotes (Fig. 3C and D). Conversely, when axenic amastigotes were converted back to promastigotes, the polysome profile graph indicated an increase in the translational activity (Fig. 3H), showing a restoration of the normal protein synthesis rate. However, phosphorylation of LdeIF2α was not detected in promastigotes that were converted back from axenic amastigotes (Fig. 3I), as shown by densitometric analysis (Fig. 3J). The expression level of stress-responsive genes, *viz*., APx (ascorbate peroxidase) and sHSP20 (small heat shock protein 20), revealed ~5- and ~1.8-fold upregulation in axenic amastigotes compared to promastigotes at the transcriptional level, respectively (Fig. 3E). Western blot analysis of *L. donovani* ascorbate peroxidase (LdApx) and sHSP20 also demonstrated upregulation by ~4-fold and ~1.8-fold, respectively, in amastigotes compared to promastigotes, as analyzed densitometrically (Fig. 3F and G), and α-tubulin was used as a loading control.

Docking study of GSK2606414 as a PERK inhibitor. Phosphorylation of eIF2α is driven by various stress-responsive eIF2α kinases activated under specific stress conditions. In *Leishmania* parasites, the presence of PERK-like eIF2α kinases has been reported (17, 18). A previous study showed that the compound GSK2606414 functions as a PERK inhibitor (22). To investigate the ability of GSK2606414 to inhibit *L. donovani* PERK (LdeK), the tertiary structure was required. In the absence of the crystal structure, we modeled LdeK. Of five different models of LdeK generated by using the I-TASSER server, the second model revealed the lowest discrete optimized protein energy (DOPE)

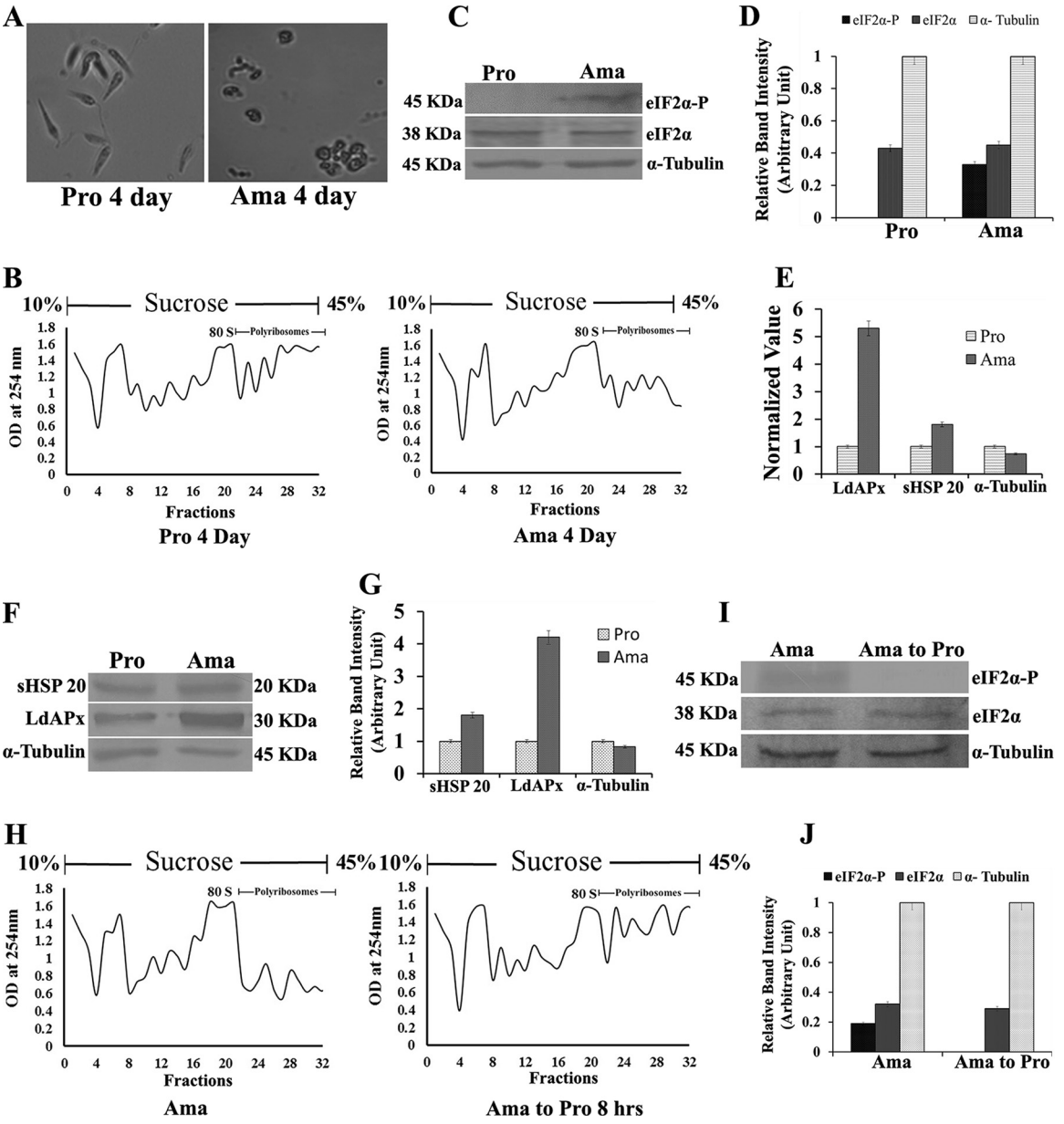

FIG 3 LdeIF2α phosphorylation during promastigote-to-amastigote transformation decreases global translation. (A) Promastigote-to-amastigote differentiation of *L. donovani* promastigotes. *L. donovani* promastigotes (Pro 4 Day) and axenic amastigotes (Ama 4 Day) under high-power magnification were grown in M199 medium at 37°C at pH 5.5 for 4 days on average (first passage). The majority of *L. donovani* promastigotes transformed into amastigote-like structures after 4 days of growth under the above-mentioned conditions. Elevated temperature and low pH are the major factors triggering promastigotes to differentiate into amastigotes within the phagolysosome of the host macrophage. (B) Polysome profile of both promastigotes and axenic amastigotes. Lysates were fractionated by 10% to 45% sucrose density ultracentrifugation, and the absorbance was read at 254 nm. (C) Western blot analysis to detect the phosphorylation status of LdeIF2α in promastigotes and amastigotes. *L. donovani* cells were lysed, and lysates were immunoreacted with rabbit polyclonal anti-eIF2α (pS51)-phosphospecific antibody (eIF2α-P). Protein loading was monitored by using an anti-*Leishmania*-specific eIF2α antibody raised in mice. (D) Densitometry for Western blot bands from the above-described experiment. (E) Expression levels of the stress-responsive genes *LdApx* (*L. donovani* ascorbate peroxidase gene), *sHSP20* (small heat shock protein 20 gene) and α-*Tubulin* in promastigotes and amastigotes at the transcriptional level. (F) Western blot analysis showing LdApx, sHSP20, and α-tubulin in promastigotes and amastigotes at the protein level. (G) Densitometric analysis of Western blots of LdApx, sHSP20, and α-tubulin. (H) Polysome profile pattern of reversion of *L. donovani* axenic amastigotes to promastigotes. Axenic amastigotes were grown in M199 medium at 37°C at pH 5.5 and transferred to M199 medium at 25°C at pH 7.3 for 8 h, and the phosphorylation status of LdeIF2α was observed at reversion. (I) Western blot analysis of the phosphorylation status of LdeIF2α during amastigote-to-promastigote reversion (after 8 h), with α-tubulin as an internal control. (J) Band intensity analysis using densitometry. Data represent results from one of three separate experiments.

score (−66,600.18) and was considered for further study. The Φ/Ψ distribution of the backbone conformational angle for each residue of the chosen structure revealed 93.7% of residues in the most favored region and an additional allowed region and 2.2% of residues in the generously allowed region, whereas only 4.1% of residues fell in the disallowed region. Validation of the modeled protein by using the ProSA-web server revealed a *Z* score of −6.84 (Fig. 4A). The ERRAT plot showed that 86.46% of residues were below the error value cutoff limits. The prepared model was then processed for molecular dynamics (MD) simulation on a 20-ns time scale under explicit solvent conditions. Figure 4B shows the all-atom root mean square deviation (RMSD) of the modeled system against the time scale. The docking experiments suggested that two amino acid residues, namely, Leu544 and Arg565, formed hydrogen bonds with the ligand molecule (Fig. 4C). The protein-ligand complex, as obtained from Glide v9.10, was processed for MD simulations with Newton's laws of motion under explicit solvent conditions. Figure 4D contains the hydrogen-bonding profile of the ligand protein complex against the time scale. BLASTP (BLAST2seq) analysis of leishmania and human PERK revealed a very low sequence identity, but the lipophilic volume bounded by the side chains of C-α helix residues A643 and Y653 was found to be conserved with *Leishmania* PERK. Also, V639, K621, and M887 were conserved in both species (Fig. 4E). A dose-response curve for different concentrations of GSK2606414 in relation to the percent viability of promastigotes showed that 95% of the promastigotes were viable at concentrations of up to 40 nM (Fig. 4F), which is nonsignificant compared to UNS parasites.

GSK2606414 inhibits LdeIF2α phosphorylation. To further explore the effect of GSK2606414 on the LdeIF2α phosphorylation status, *L. donovani* promastigotes were exposed to elevated temperature and acidic pH (37°C and pH 5.5, respectively) with or without GSK2606414 (30 nM). Western blotting using anti-phosphospecific eIF2α antibody (pS51) showed that the degree of LdeIF2α phosphorylation decreased by ~2.0-fold in the presence of GSK260414, as shown by immunoblotting (Fig. 4G) and densitometry scanning (Fig. 4H). Similarly, the effect of GSK2606414 on mammalian cells was also studied. Mouse PECs were exposed to thapsigargin in the absence or in the presence of GSK2606414. Western blot analysis detects the phosphorylation of mouse eIF2α in the absence of GSK2606414; however, no band was detected in thapsigargin-exposed PECs in the presence of GSK2606414 (Fig. 4I), showing the inhibition of mammalian eIF2α phosphorylation by GSK2606414. Thus, the results from this study suggest that GSK2606414 inhibits stress-induced LdeIF2α phosphorylation.

Impaired LdeIF2α phosphorylation reduces antioxidant levels and leads to accumulation of ROS, leading to decreased parasite viability in an oxidative environment. Thiols are the major antioxidants involved in counterbalancing oxidative stress. The total intracellular reduced thiol content under oxidative pressure was found to be higher in H_2O_2-treated parasites than in parasites exposed to H_2O_2 plus GSK260414 or the thiol metabolic pathway inhibitor buthionine sulfoximine (BSO), difluoromethylornithine (DFMO), or both. The total amount of reduced thiol was found to be ~1.3-fold lower ($P < 0.05$) in parasites subjected to H_2O_2 along with GSK260414 than in those subjected to only H_2O_2 (Fig. 5A), whereas a comparatively higher level of reduced thiol was observed in UNS parasites or parasites incubated with GSK260414 without any oxidative pressure. Intracellular ROS generation as analyzed spectrofluorimetrically by using H_2DCFDA dye showed ~2.4-fold-higher ROS levels in parasites exposed only to H_2O_2 than in UNS parasites. However, parasites incubated with GSK260414 with H_2O_2 exposure showed ~1.3-fold-higher levels of ROS accumulation than those in parasites exposed to H_2O_2 ($P < 0.05$) (Fig. 5B). Fluorescence microscopic analysis of labeled parasites confirmed ROS generation under different stress conditions, as shown in Fig. 5C. These findings clearly suggest that the inhibition of stress-induced LdeIF2α phosphorylation leads to ROS accumulation. Additionally, real-time PCR analysis of the expression of genes involved in redox homeostasis, *viz*., ornithine decarboxylase (Odc), glutathione synthetase (Gss), trypanothione synthetase

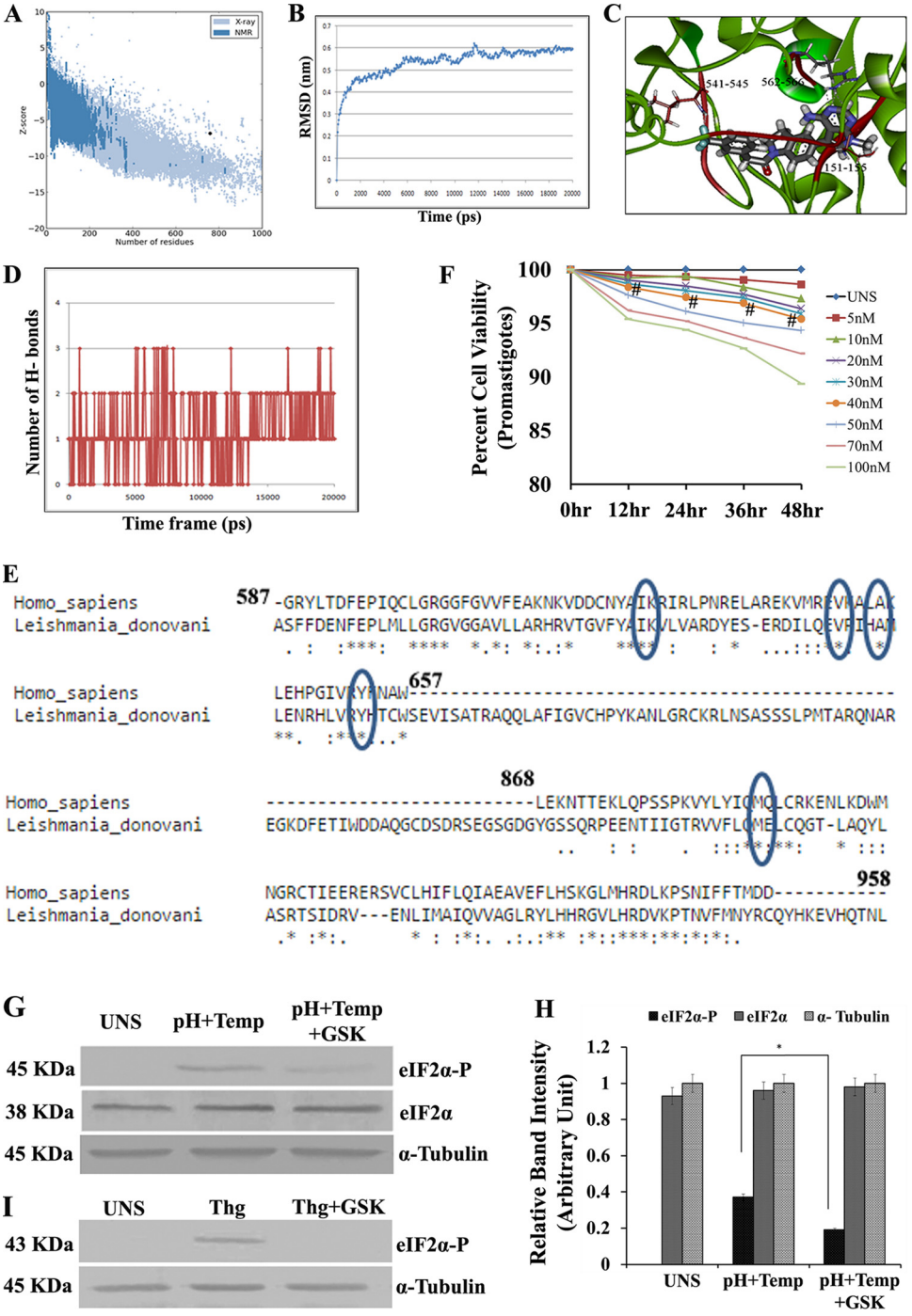

FIG 4 Docking study of GSK2606414 as a PERK inhibitor. (A) Pro SA-web server. Plot validation of the modeled protein with the ProSA-web server showed a *Z* score of −6.84. The ERRAT plot showed that 86.46% of residues were below the error value cutoff limits. (B) An MD simulation was conducted for the modeled system in explicit solvent by using GROMACS 4.0.3. The RMSD in the C-α backbone atom in the *L. donovani* eIF2α kinase protein (LdeK) for up to 4 ns after the 20-ps model attains its maximum stability is shown. lsq, least squares. (C) Study of docking of GSK260414 (inhibitor of PERK enzymes) with the *L. donovani* eIF2α kinase protein. The result obtained from DS2.5 and Glide v9.10 suggest that the interaction between Leu151-Ser155, Arg541-Asp545, and Arg562-Arg566 may play a key role in the inhibition of *L. donovani* eIF2α kinase (LdeK). (D) Profile of H-bonding between GSK2606414 and the PERK kinase domain (LdeK) gene. (E) Comparison of *L. donovani* PERK and mammalian PERK (human) by protein sequence alignment. (F) Dose-response curve for different concentrations of GSK2606414. At concentrations of up to 40 nM, the percent viability of untreated promastigotes was above 95% compared to untreated parasites (UNS) (# denotes nonsignificant data sets compared with untreated ones). (G) Western blotting to determine the phosphorylation status of LdeIF2α under unstressed conditions, pH and temperature stress (pH+Temp), and pH and temperature stress after GSK2606414 (30 nM) treatment (pH+Temp+GSK). α-Tubulin was used as a control. (H) Densitometric analysis of band intensities. (I) Western blotting to determine the phosphor-

(Continued on next page)

(Trys), γ-glutamyl cysteine synthetase (γ-Gcs), trypanothione reductase (Tryr), and ascorbate peroxidase (Apx), showed ~2- to ~3-fold upregulation in promastigotes exposed to oxidative stress compared to the levels in unexposed control parasites. However, the fold increase in the level of redox homeostasis genes was observed to be lower in parasites exposed to H_2O_2 plus GSK (Fig. 5D). Furthermore, analysis of percent cell viability after exposure to H_2O_2 (200 μM) alone or in the presence of GSK2606414 showed ~74% cell viability for parasites treated with H_2O_2 alone compared to that for unstressed parasites and ~58% cell viability for parasites treated with H_2O_2 plus GSK260414 ($P < 0.05$) (Fig. 5E). Parasites incubated with GSK2606414 alone were used as controls and did not show any significant decrease in viability. These results confirmed that stress-induced LdeIF2α phosphorylation helps the parasites to adapt to and survive in an oxidative environment.

Inhibition of LdeIF2α phosphorylation under drug pressure reduces parasite viability. As results from previous experiments showed that drug-generated ROS are also capable of inducing LdeIF2α phosphorylation, we estimated parasite viability under drug pressure in the presence of GSK2606414. The percent viabilities of promastigotes after 48 h of exposure to SAG_{40} or SAG_{70} were 71% and 59%, respectively, whereas in the presence of GSK, viabilities were 62% and 46%, respectively. Similarly, with exposure to amphotericin B, *viz*., Amp $B_{0.03}$ or Amp $B_{0.06}$, the percent viabilities were 76% and 52%, respectively, which were further decreased significantly in the presence of GSK2606414 to 61% for treatment with Amp $B_{0.03}$ plus GSK and to 39% for treatment with Amp $B_{0.06}$ plus GSK (Fig. 5F). Untreated parasites were used as controls. Thus, these results suggest that stress-induced LdeIF2α phosphorylation favors parasite survival under drug pressure.

Inhibition of LdeIF2α phosphorylation hampers promastigote-to-amastigote transformation and decreases parasite viability. To elucidate whether LdeIF2α phosphorylation is a prerequisite for parasite transformation of promastigotes to infective amastigotes, *L. donovani* promastigotes were subjected to both temperature and pH stress (37°C and pH 5.5, respectively) in the presence or absence of GSK2606414. Microscopic investigation revealed that parasites treated with GSK2606414 did not show significant changes in morphology compared to parasites exposed to high-temperature and low-pH stress (37°C and pH 5.5, respectively) for 48 h. In the presence of the inhibitor (GSK260414), the elongated promastigotes had intact flagella and did not transform to a round shape (Fig. 6A) compared to control untreated parasites. Furthermore, polysome analysis showed no significant change in the polysome level in GSK260414-treated parasites exposed to heat and pH stress compared to those in unstressed parasites (Fig. 6B). To confirm the initiation of the differentiation process in promastigotes, Western blot analysis of the amastigote-specific A2 protein was performed. As expected, higher expression levels of the A2 protein were detected in promastigotes exposed to heat and pH stress than in unstressed promastigotes. However, parasites treated with the inhibitor (GSK2606414) under identical heat and pH stress conditions showed markedly lower expression levels of A2 than those in stressed parasites without the inhibitor (Fig. 6C). In addition, to address whether the inhibition of LdeIF2α phosphorylation under stress affects parasite viability, the percent cell viability of *L. donovani* promastigotes subjected to high-temperature and low-pH stress in the absence or presence of GSK260414 was estimated. Parasites subjected to heat and pH stress in the absence of GSK260414 showed 32% cell viability. However, parasites exposed to identical stress in the presence of GSK2606414 showed only 17% cell viability ($P < 0.05$) (Fig. 6D).

FIG 4 Legend (Continued)
ylation status of mammalian eIF2α (mouse PECs) under unstressed conditions, with thapsigargin treatment (1 μM), and in PECs treated with thapsigargin along with GSK2606414 (30 nM) (Thg+GSK) to show the effect of GSK2606414 on mammalian PERK. α-Tubulin was used as a loading control. Data displayed here represent results from one of three separate experiments.

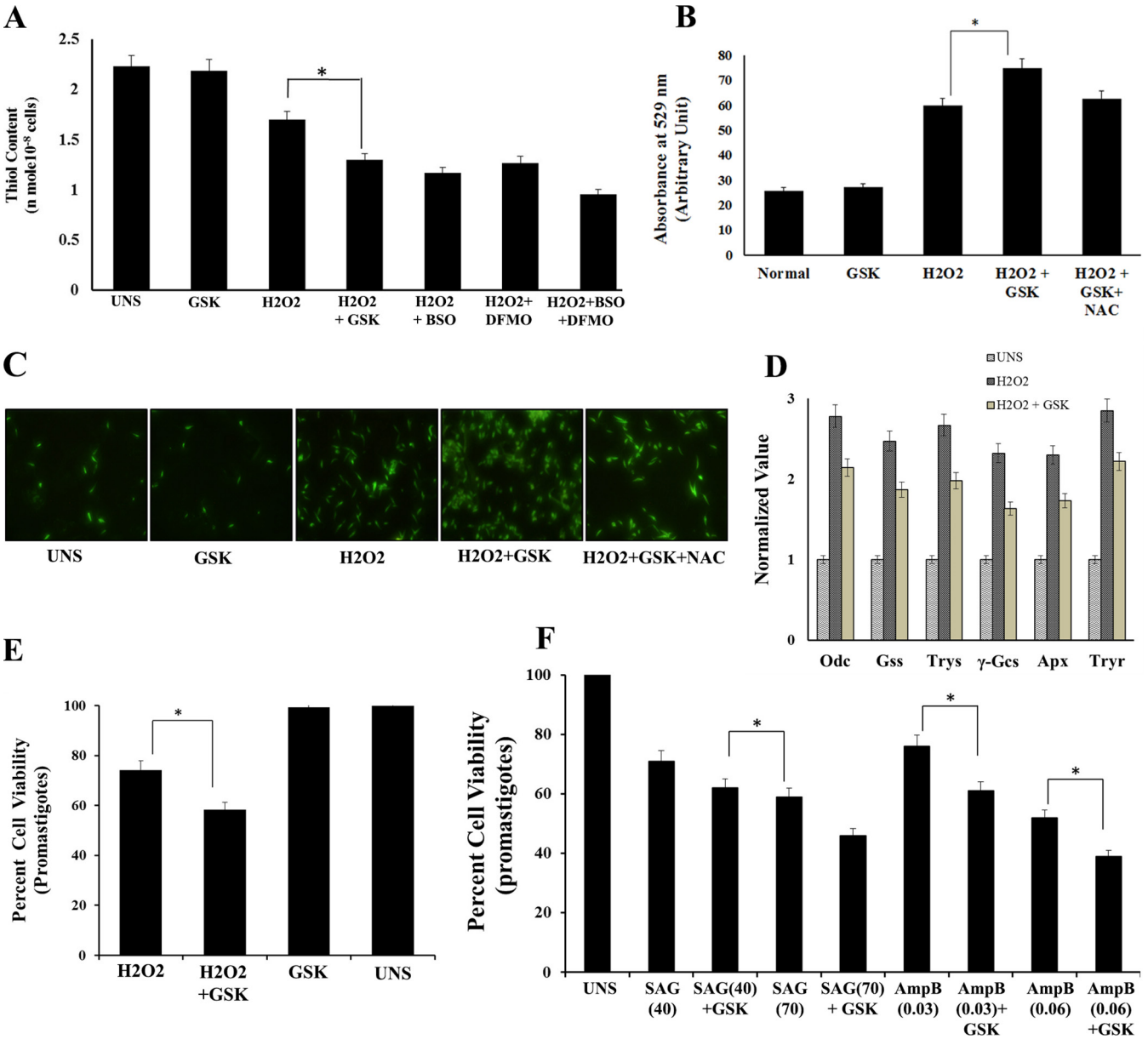

FIG 5 Inhibition of LdelF2α phosphorylation leads to accumulation of ROS and decreased antioxidant levels, leading to reduced parasite viability under conditions of oxidative stress. (A) Analysis of reduced intracellular thiol levels in untreated (UNS) *L. donovani* parasites or parasites incubated with GSK260414 (GSK) or treated with 200 μM H_2O_2 or the combination of H_2O_2 plus GSK260414 or inhibitors of the thiol metabolic pathway, including H_2O_2 plus BSO, H_2O_2 plus DFMO, or a combination of H_2O_2, BSO, and DFMO, after 4 h of treatment. The reduced intracellular thiol level was found to be lower in parasites subjected to H_2O_2 treatment along with GSK260414 than in parasites treated without GSK. (B) Graph showing the presence of intracellular ROS at 4 h for untreated *L. donovani* promastigotes or parasites incubated with GSK260414, treated with H_2O_2, incubated with GSK260414 and treated with H_2O_2, or incubated with NAC and GSK and subjected to H_2O_2 treatment (H_2O_2+NAC+GSK). ROS generation was determined spectrofluorimetrically by using H_2DCFDA dye. Values shown are the means and SDs of results from three independent experiments. (C) Fluorescence microscopic images of parasites incubated with H_2DCFDA to show ROS generation under the above-mentioned stress conditions after 4 h of stress treatment. (D) Real-time PCR analysis of genes involved in redox homeostasis. Shown are the relative expression levels of ornithine decarboxylase (Odc), glutathione synthetase (Gss), trypanothione synthetase (Trys), γ-glutamyl cysteine synthetase (γ-Gcs), ascorbate peroxidase (Apx), and trypanothione reductase (Tryr) of *L. donovani* with respect to values for α-tubulin (control). The expression level was found to be upregulated by ~2- to ~3-fold when promastigotes were exposed to H_2O_2-induced oxidative stress compared to untreated controls. The expression levels of redox homeostasis genes were found to be low in parasites incubated with GSK2606414 and subjected to oxidative stress. (E) Percent cell viability of *L. donovani* promastigotes subjected to oxidative stress generated due to H_2O_2 treatment or in the presence of GSK2606414 and under H_2O_2 stress along with GSK2606414 after 4 h of treatment. (F) Percent viability at 48 h of promastigotes exposed to SAG_{40}, SAG_{70}, SAG_{40} plus PERK, SAG_{70} plus PERK, Amp $B_{0.03}$, Amp $B_{0.06}$, Amp $B_{0.06}$ plus PERK, or Amp $B_{0.03}$ plus PERK. In these cases, untreated parasites were used as controls. Values are the means and SDs of results from three independent experiments, and significant differences are indicated by * ($P < 0.05$).

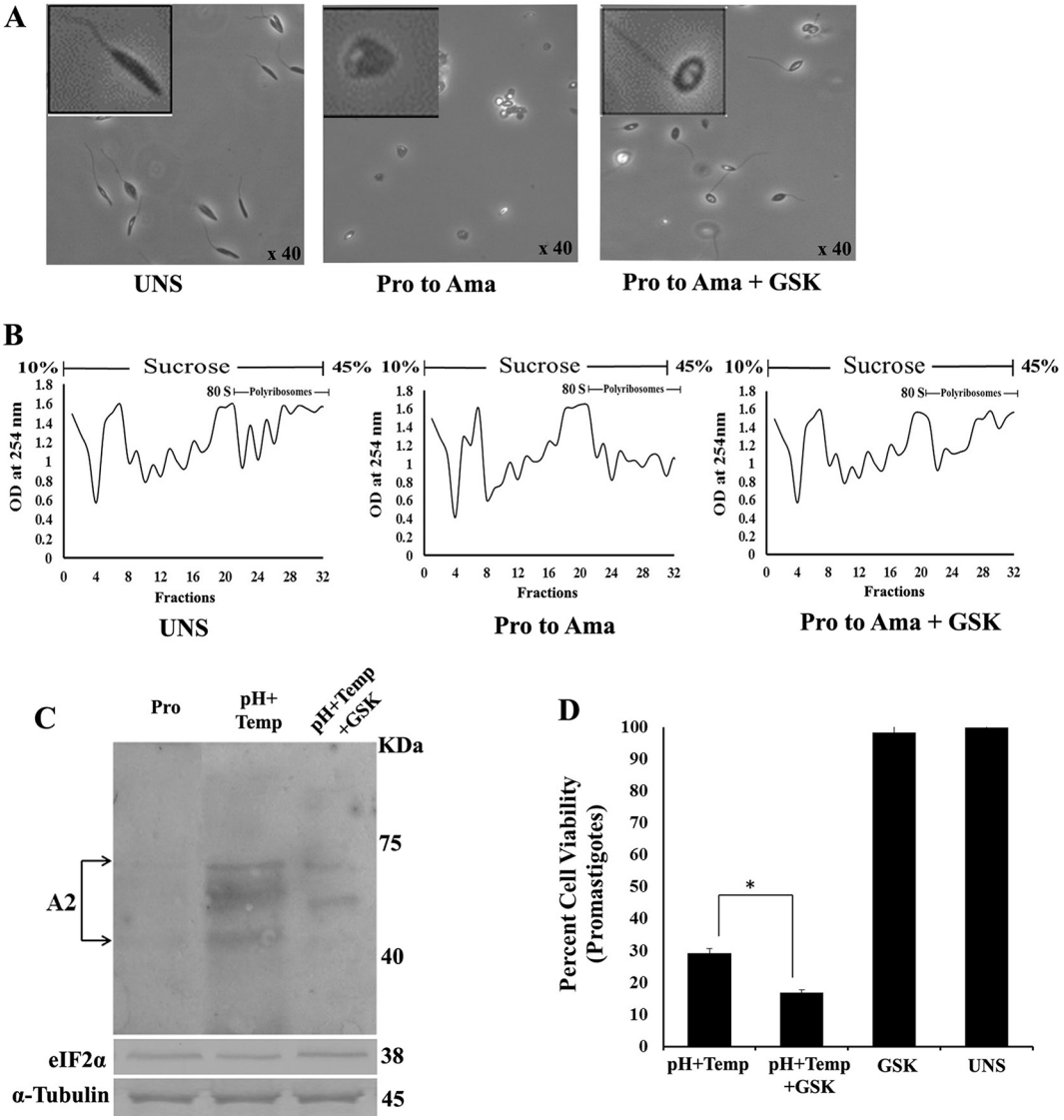

FIG 6 Impaired stress-induced LdeIF2α phosphorylation hampers promastigote-to-amastigote transformation and reduces parasite viability. (A) Phase-contrast images showing morphological changes during transformation from promastigotes (Pro) to amastigotes (Ama) in the absence or presence of GSK2606414. (B) Polysome profiles of *L. donovani* promastigotes grown under unstressed conditions and axenic amastigotes and promastigotes subjected to 48 h of high temperature and low pH (37°C and pH 5.5) with GSK2606414 (pH+T+GSK) or without GSK2606414 treatment. (C) Western blot analysis of *L. donovani* protein lysates with monoclonal anti-A2 antibody to determine the expression levels of the A2 protein in unstressed promastigotes or promastigotes subjected to 48 h of high temperature and low pH (37°C and pH 5.5, respectively) (pH+T) and promastigotes subjected to 48 h of high temperature and low pH (37°C and pH 5.5, respectively) along with GSK2606414. LdeIF2α and α-tubulin were used as loading controls in the same experiment. Data shown here are representative of data from three independent experiments with similar results. (D) Percent cell viability of *L. donovani* promastigotes subjected to combined exposure to high-temperature (37°C) and low-pH (pH 5.5) stress or high-temperature (37°C) and low-pH (pH 5.5) stress with GSK2606414 or in the presence of GSK2606414 only, monitored by MTT survival assays at 48 h.

Inhibition of LdeIF2α phosphorylation reduces infection rates. To explore the role of LdeIF2α phosphorylation in *Leishmania* infection, we determined the infection rate of parasites pretreated with or without GSK2606414 for 3 h on PECs isolated from mice. The results showed a ~40% reduction in infection ($P < 0.05$) for GSK2606414-treated parasites compared to untreated parasites. For UNS parasites, 77 out of 100 macrophages were infected at 48 h postinfection, but for GSK260414-treated parasites, only 46 out of 100 macrophages were infected (Fig. 7B and C). Uninfected PECs were used as a negative control (Fig. 7A). Figure 7D shows a graphical representation of the

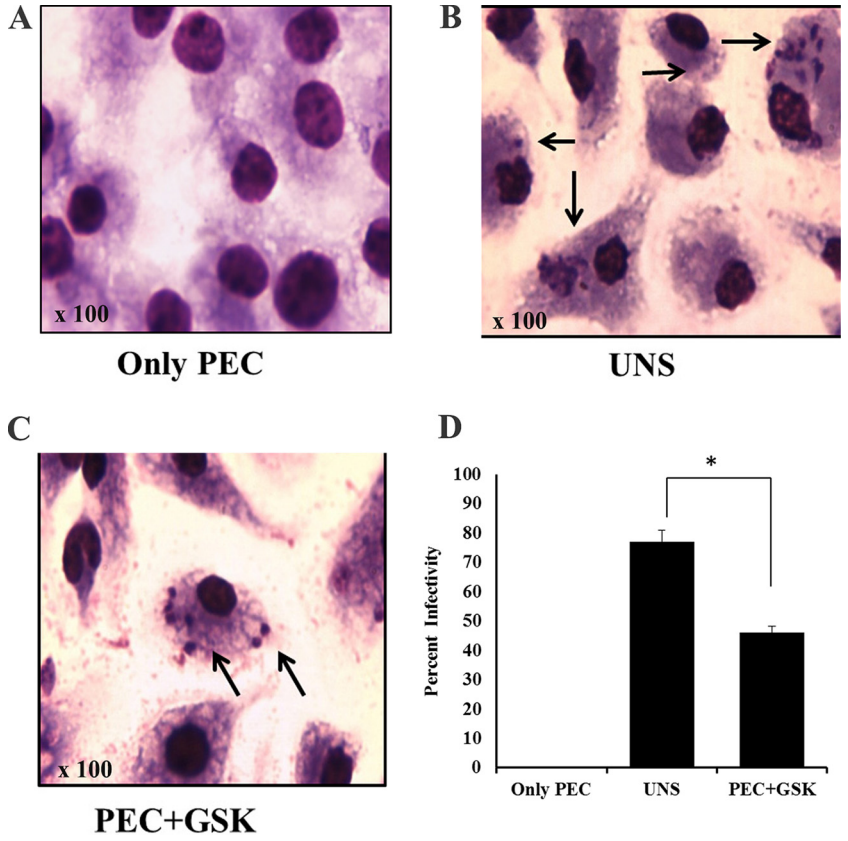

FIG 7 Inhibition of LdeIF2α phosphorylation reduces the infection rate. (A) Uninfected PECs were used as a negative control. (B and C) Mouse PECs were isolated after stimulation with a 4% starch solution and infected with normal *L. donovani* promastigotes (UNS) (B) or with promastigotes preincubated with GSK2606414 for 3 h and washed in PBS prior to infection (C). (D) The infection rate was estimated by counting the infected macrophages per 100 macrophages after 48 h. Significant differences are indicated by * ($P < 0.05$).

results. Thus, these results yield conclusive evidence that stress-induced LdeIF2α phosphorylation has a role in virulence.

DISCUSSION

Translation control via phosphorylation of eIF2α is a central mechanism in eukaryotes to combat stress by reconfiguring gene expression (23). In unicellular protozoan parasites, eIF2α phosphorylation under stress may induce the conversion of one form into another, which is distinguishable at morphological and biochemical levels (24). Cycling between cold-blooded insect vectors and warm-blooded mammalian hosts is typical for most parasitic protozoa, including *Leishmania*.

The elevated temperature and acidic pH that resemble the phagolysosomal environment of host macrophages induced the phosphorylation of LdeIF2α, leading to decreased global translation levels and the upregulation of stress-responsive genes such as LdApx and sHSP20 (Fig. 3E and F). This is consistent with many previous reports showing that elevated temperature and/or acidic pH induced the mRNA expression of several stress-responsive genes, including LdApx and sHSP20 (1, 25–27), favored by reduced translation during amastigote differentiation, allowing parasites to conserve energy while reconfiguring the expression of specific sets of genes necessary for their survival in the mammalian host (28). It has been shown that elevated temperature and acidic pH induce the phosphorylation of eIF2α and trigger the differentiation of *L. infantum* by decreasing global translation and enhancing the relative expression levels of stress-responsive proteins, enabling the parasite to adapt according to persisting physiological conditions inside the phagolysosomal compartment of host macrophages

(12, 29). In the amastigote stage, the phosphorylated state of LdeIF2α is maintained to ensure low energy expenditure on metabolism while residing in the nutrient-deficient hostile conditions of macrophages.

Being an intracellular parasite, *Leishmania* is exposed to oxidative stress throughout its mammalian life cycle, starting from its entry inside macrophages and continuing throughout its residence inside the phagolysosomal compartment (30, 31). During the early stages of infection, the parasites have to combat ROS generated by the respiratory burst of macrophages for successful invasion (32). The conditions used for axenic transformation of *Leishmania* promastigotes to amastigotes, *viz*., low pH and elevated temperature, also generate significant amounts of ROS accompanied by drastic morphological and physiological changes (33). Recently, it was reported that the iron uptake-dependent regulation of ROS-mediated signaling plays a central role in triggering the differentiation of noninfective *L. amazonensis* promastigotes into the highly virulent amastigote forms (34). Thus, ROS are gaining widespread acceptance as important signaling molecules in the physiology of *Leishmania*. In this context, the observed LdeIF2α phosphorylation by ROS generated under various stress conditions such as H_2O_2 or heat/pH stress or by the antileishmanial drugs SAG and Amp B (Fig. 2A) shows that, irrespective of the source, ROS phosphorylates LdeIF2α, and its phosphorylation may act as one of the key mediators of ROS-dependent changes at the molecular level to initiate the differentiation of *L. donovani* promastigotes into amastigotes.

Phosphorylation of eIF2α is mediated by different stress-responsive eIF2α kinases depending on the stress conditions, which, initially activated by autophosphorylation, in turn phosphorylates eIF2α (13). In *Leishmania*, only the PERK-type eIF2α kinase has been predicted until now. It is a classical serine-threonine kinase which undergoes autophosphorylation and is activated by the unfolded-protein response (UPR), a signal transduction pathway that coordinates cellular adaptation to microenvironmental stresses, including hypoxia, nutrient deprivation, and changes in the redox status (35, 36). Protozoan parasites have eIF2α kinases that share the basic mechanistic features of their mammalian counterparts but have adapted different regulatory domain configurations, suggesting that the parasite eIF2α kinases may trigger translational control in response to different stress signals than those reported for mammals (24). Also, approaches to generate a PERK$^{-/-}$ mutant in the *Leishmania* diploid genome have so far been unsuccessful. As PERK is essential for parasite growth, it is a key target kinase molecule for inhibition studies (17).

The PERK-eIF2α signaling pathway plays a significant role in protection against ROS damage by altering the antioxidant level (19, 20). With H_2O_2 treatment, promastigotes incubated with GSK260414 showed high levels of ROS accumulation (Fig. 5B and C) and decreased antioxidant levels (Fig. 5A) as a consequence of the downregulation of genes involved in the maintenance of redox homeostasis (Fig. 5D). This strongly indicates the role of stress-induced LdeIF2α phosphorylation in detoxification and protection against ROS. Furthermore, the presence of GSK260414 decreased parasite viability significantly under stress, suggesting the promising role of LdeIF2α in parasite survival under stress (Fig. 5E). LdeIF2α phosphorylation upon exposure to SAG and Amp B and decreased parasite viability upon exposure to the combination of GSK and the drug (Fig. 5F) showed that drug-generated ROS can also activate the stress-responsive pathway, playing an important role in survival under drug pressure. Given the crucial role of ROS in initiating signaling mechanisms during parasite differentiation (37) as well as their importance for parasite survival during infection, the role of LdeIF2α phosphorylation in the persistence and virulence of *L. donovani* parasites seems inevitable. During ROS exposure, LdeIF2α phosphorylation may be a key trigger for the regulation of a plethora of downstream proteins, culminating in the reprogrammed parasite's metabolic machinery, which is capable of apt elimination of the oxidative stress.

Transformation from the promastigote form to the amastigote form under conditions of elevated temperature and acidic pH is an adaptation of the parasite to the unfavorable conditions of the phagolysosomal compartment, accompanied by a num-

ber of morphological and biochemical changes. These changes include the conversion of elongated, motile, and flagellated promastigotes into round, nonmotile, and aflagellated amastigotes and the expression of genes of the A2 family, which are amastigote-specific genes used as an indicator of the initiation of the transformation process (38, 39). The acidic-pH- and high-temperature-induced transformation of *L. donovani* promastigotes into axenic amastigotes was associated with LdeIF2α phosphorylation and ROS generation, indicating a link between them, in accordance with our previous observation of LdeIF2α phosphorylation by H_2O_2-generated ROS. Moreover, the delay/inhibition of differentiation by GSK2606414 treatment confirmed the role of LdeIF2α phosphorylation in the differentiation process, and associated factors such as the lack of a change in morphology, the lack of a significant decrease in the polysome level, and decreased A2 expression levels compared to those in normal or untreated parasites further validate our observations (Fig. 6A to C). Consequently, decreased cell viability was observed in parasites subjected to an impaired differentiation process (Fig. 6D). Furthermore, data from an *ex vivo* infection study of mouse PECs, which showed a decreased infectivity rate for parasites pretreated with GSK260414 (Fig. 7), strongly support the fact that ROS-mediated phosphorylation of LdeIF2α is an important event in the differentiation of *Leishmania* promastigotes into an amastigote form and, hence, the establishment of infection.

Hence, starting from the beginning of invasion in the mammalian host, the induction of LdeIF2α phosphorylation enables the parasite to adapt to the stressed environment through modification of translation flux toward stress-responsive genes and finally to the amastigote stage and its maintenance, adapted to survive inside the harsh phagolysosomal compartment (Fig. 8).

Overall, we conclude that stress-induced phosphorylation of LdeIF2α is a crucial event in the life cycle of *L. donovani* through (i) transformation of the motile promastigote form into the nonmotile amastigote form; (ii) decreased global translation and upregulation of stress-responsive genes during transformation or in the amastigote form, which indicates the adaptive response of parasites to conserve energy and divert it toward the minimum essential pathways required for survival, exemplified by thiol redox metabolism (27, 40); and (iii) use of the pentose phosphate pathway (41) for coping with oxidative stress and energy generation (37), respectively, while converting the more active form into the low-metabolic amastigote form. ROS accumulation, decreased viability, and a drastic decrease in the infectivity rate upon the inhibition of stress-induced LdeIF2α phosphorylation emphasize the importance of this stress-responsive pathway. Moreover, drug-induced LdeIF2α phosphorylation indicates its possible involvement in drug unresponsiveness and resistance, as the above-described drugs follow the same mode of action for parasite clearance (42).

Indeed, results from this study suggest directions for new therapeutic options. Specific inhibitors targeting this stress-responsive pathway may serve as potential candidates for antileishmanial drugs, which are urgently needed given that resistance against traditionally used antileishmanial drugs is a common phenomenon.

MATERIALS AND METHODS

***Leishmania* cell culture.** Promastigotes of *Leishmania donovani* AG83 clones (MHOM/IN/1983/AG83) were used in all experiments. The promastigotes were grown at 25°C in 25-cm^2 flasks (Nunc) in fresh M199 medium (Gibco) supplemented with 10% fetal bovine serum (FBS) (Gibco). Cultures were allowed to reach stationary phase (5 to 6 days postinoculation), as determined by growth curve analysis (data not shown), prior to inoculation into fresh medium. The infectivity of the clone was maintained regularly in Syrian golden hamsters. For the generation of axenic amastigotes, late-stationary-phase promastigotes were inoculated in M199 medium supplemented with 20% serum in 25-cm^2 ventilated flasks and grown at 37°C at pH 5.5 with 5% CO_2 for an average of 5 days for promastigote-to-amastigote differentiation in a cell-free culture; maintenance of axenic amastigotes was carried out as described previously (43). For *in vitro* generation of oxidative stress, H_2O_2 (200 μM) (Merck GmbH, Darmstadt, Germany) was added to the promastigote culture, suspended in fresh medium, and incubated at 25°C inside a basic oxygen demand (BOD) incubator (41). Due to the short half-life of H_2O_2, the treatment time was limited to 4 h. SAG and Amp B treatments were given for 8 h at two different doses, *viz.*, 40 μM (SAG_{40}) and 70 μM (SAG_{70}) for SAG and 0.060 μM (Amp $B_{0.06}$) and 0.030 μM (Amp $B_{0.03}$) for amphotericin B, based on the 50% lethal doses (LD_{50}s) of the drugs, as described previously (44). The treatment time for deducing

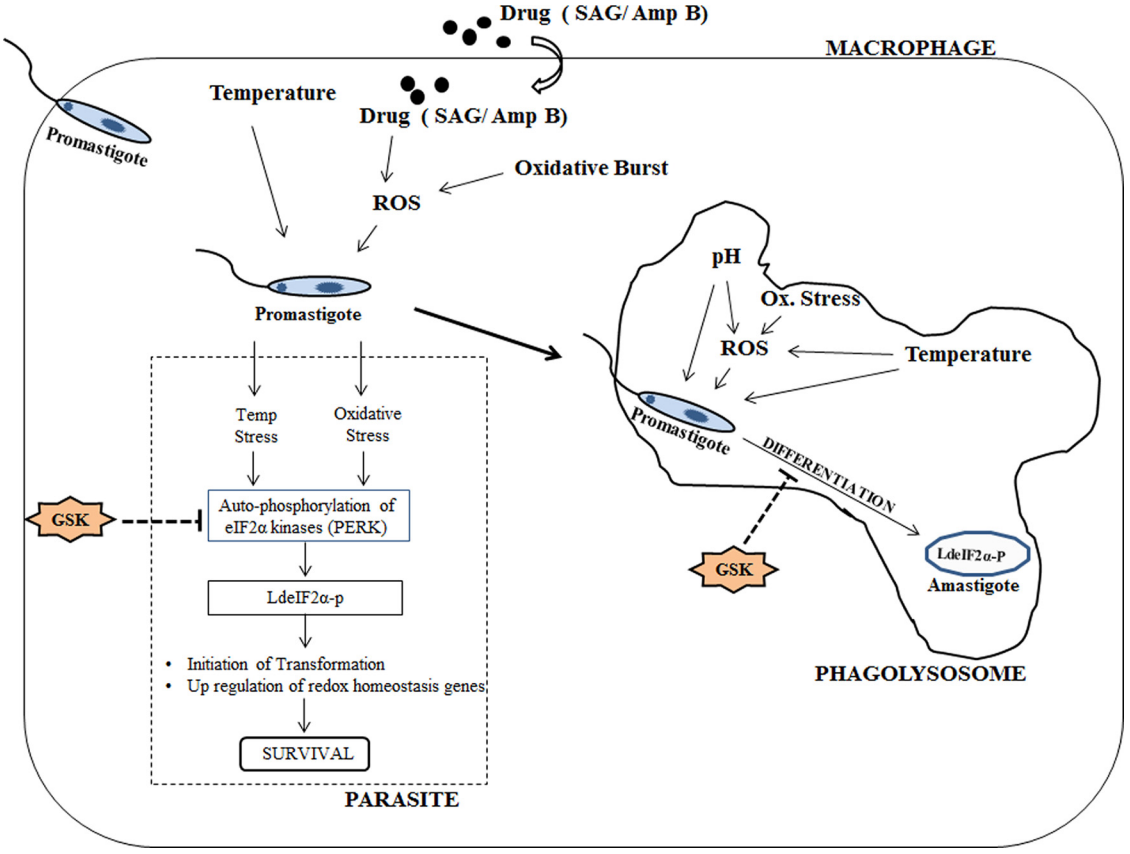

FIG 8 Hypothetical model showing events during parasite entry inside macrophage in relation to stress-induced phosphorylation of LdeIF2α. As the parasite enters the macrophage, elevated temperature and ROS generated by an oxidative burst as a consequence of the host immune response or via administered drugs such as SAG or Amp B induce LdeIF2α phosphorylation through autophosphorylation of stress-responsive LdeIF2α kinases (PERK), which in turn decreases the global translation rate, providing the chance to upregulate redox homeostasis genes for parasite survival and also initiating promastigote-to-amastigote differentiation. Inside the phagolysosomal compartment, the cumulative effect of elevated temperature, acidic pH, and ROS brings about the transformation of promastigotes into amastigotes and stabilizes the nonmotile form by maintaining LdeIF2α phosphorylation, enabling parasites to adapt to the harsh environment. However, inhibition of stress-induced LdeIF2α phosphorylation due to GSK2606414 (GSK)-mediated blockage of autophosphorylation of LdeIF2α kinases (PERK) prevents the initiation of this stress-responsive pathway in parasites, leading to reduced survival and infectivity.

LD_{50}s was kept well below 48 h to ensure that parasite viability is not significantly affected upon treatment.

Western blotting. Western blot assays were conducted to determine phosphorylation under stress conditions. Briefly, *Leishmania* promastigotes (1×10^7 cells/ml) were cultured in 24-well plates and treated with H_2O_2-amphotericin B-SAG or subjected to elevated temperature and acidic pH (37°C and pH 5.5, respectively) for the stipulated periods of time. Treated cells were washed twice with phosphate-buffered saline (PBS), resuspended, and lysed with a Dounce homogenizer in lysis buffer (10 mM Tris-HCl [pH 7.4], 150 mM NaCl, 10 mM $MgCl_2$, 0.5% IGEPAL, 1 mM PMSF [phenylmethanesulfonyl fluoride], 1× protease inhibitor cocktail [Merck], 1× PhosStop [Roche]). *Leishmania* lysates were centrifuged at 13,000 × *g* for 15 min at 4°C, and the clear supernatant was collected in a cryotube. Twenty-five milligrams of total protein lysates was loaded onto 10% SDS-PAGE gels (12). The proteins from the gels were transferred onto a polyvinylidene difluoride (PVDF) membrane (Roche) according to the manufacturer's instructions. The membrane was blocked for 60 min in Tris-buffered saline (TBS) with 5% nonfat dry skim milk for anti-LdeIF2α or 5% bovine serum albumin (BSA) for anti-A2 antibodies, prior to the addition of the first antibody. Mouse polyclonal antisera raised against *L. donovani* eIF2α (data not shown) and anti-A2 antibody (kindly provided by Greg Matlashewski, McGill University) were used at 1:1,000 dilutions. For the detection of LdeIF2α phosphorylation, blocking was performed overnight (O/N) at 4°C in 5% BSA, prior to incubation for 2 h at room temperature (RT) in 1% BSA, and rabbit polyclonal anti-eIF2α (human pS5; Cell Signaling)-phosphospecific antibody was used at a 1:1,000 dilution. Normalization was done with an α-tubulin antibody (1:1,000) (Sigma-Aldrich). Tris-buffered saline with 0.1% Tween 20 was used to wash the membranes after the blocking step. Anti-mouse or anti-rabbit antibodies that had been conjugated to horseradish peroxidase (Jackson Laboratories) were diluted at 1:10,000 in a solution containing PBS– 0.1% Tween and 5% nonfat dry skim milk and added to the membrane for 60 min. Before visualization of the signal on the membrane, three 10-min washes (PBS with 0.1% Tween 20)

were performed, and the reaction was developed with chemiluminescence by using an Amersham Hyperfilm/ECL kit (GE Healthcare) according to the manufacturer's protocol.

Polysome profiling. Polysomes are complexes formed by the association of mRNA with ribosomes, whose association is analyzed by determining the OD at 254 nm to obtain a profile that reflects the level of translation. A total of 3×10^9 *L. donovani* promastigotes in late log/stationary phase subjected to heat-acidic stress and differentiated to amastigotes in culture were incubated with 100 mg/ml of cycloheximide (Sigma) for 10 min, washed with cycloheximide-containing PBS, and lysed with a Dounce homogenizer in lysis buffer (10 mM Tris-HCl [pH 7.4], 150 mM NaCl, 10 mM $MgCl_2$, 1 mM dithiothreitol [DTT], 0.5% IGEPAL, 100 mg/ml cycloheximide, 100 U/ml RNase [Invitrogen], 1 mM PMSF, 15 μl/ml of a protease inhibitor cocktail [Merck]). *Leishmania* lysates were pelleted by centrifugation, and the supernatant (OD at 260 nm) was layered on top of a 10% to 45% linear sucrose gradient (3 ml) in gradient buffer (50 mM Tris-HCl [pH 7.4], 50 mM KCl, 10 mM $MgCl_2$, 1 mM DTT, 100 U/ml RNase inhibitor) as described previously (12, 18). Sedimentation was carried out by centrifugation with a Hitachi CP100WX instrument at 35,000 rpm for 2.15 h at 4°C, 100-μl aliquots were collected, and the absorbance was detected at 254 nm and plotted correspondingly.

Real-time PCR. Reverse transcription was performed by using 0.2 mg total RNA from untreated *L. donovani* cells or *L. donovani* cells subjected to elevated temperature (37°C) and acidic pH (pH 5.5) or H_2O_2 treatment (48 h) by using an anchored oligo(dT) primer (H-dT11M, where M represents A, C, or G; Gen-Hunter). Real-time PCR was performed with a LightCycler 480 instrument (Roche) using SYBR green chemistry (Roche). The cycling conditions were 1 cycle of 95°C for 3 min and 40 cycles of 95°C for 15 s (denaturation), 58°C for 30 s (annealing), and 72°C for 30 s (extension). The fluorescence signal was captured at the end of each cycle by using the SYBR channel (490-nm wavelength for excitation and 525-nm wavelength for emission). Results were expressed as target/reference ratios for each sample, normalized by the target/reference ratio of the calibrator. Here, the target/reference value of untreated/normal parasites was used as the calibrator, and α-tubulin was used as the reference. The primers used for real-time PCR were sense primer 5′-CGAACTGGCTTGACATGAAC-3′ and antisense primer 5′-GCAGG TGAAACTCGTGATTTG-3′ for Apx, sense primer 5′-ACATCACGAACTCGGTGTTT-3′ and antisense primer 5′-TCGTCTTGATCGTCGCAAT-3′ for α-tubulin, sense primer 5′-GAACTCCATCTCAAACTCCCC-3′ and antisense primer 5′-TCCCTAGACGAAATTGCAGC-3′ for Odc, sense primer 5′-CGAACTGGCTTGACATGAAC-3′ and antisense primer 5′-GCAGGTGAAACTCGTGATTTG-3′ for Trys, and sense primer 5′-TCTTCATTCCGCT TCTCACC-3′ and antisense primer 5′-ATGTATTGTTCTCCACACGGG-3′ for γ-Gcs (40).

Homology modeling, docking, dynamics, and simulation study. Prediction of the tertiary structure was preceded by homology modeling, since crystal structures of the targeted protein are unavailable. The full-length amino acid sequence of the *Leishmania donovani* eIF2α kinase protein (LdeK) (GenBank accession number EU194953.1) was downloaded from the Universal Protein Resource Database (http://www.uniprot.org/). The low percentage of sequence identity in the homologous PDB structures may not provide robust models for protein structure. A BLASTP search against the PDB database returned no results for homologous crystal structures, and thus, we relied upon the Zhang laboratory I-TASSER server (http://zhanglab.ccmb.med.umich.edu/I-TASSER/). Among the five models generated by the I-TASSER algorithm, the model with the lowest DOPE score was selected and verified by using the Profile 3D (DS.2.5) profile analysis method. The stereochemical property of the predicted model was investigated with the Structural Analysis and Verification Server (SAVES) (http://nihserver.mbi.ucla.edu/SAVES/), and the quality of the selected model was analyzed by using the ProSA-web server (45). The initial three-dimensional (3D) structure of the *Leishmania donovani* eIF2α protein obtained from homology modeling was optimized by using MD simulation according to a previously described protocol (46). The final MD was carried out for 20,000 ps (20 ns) with particle mesh Ewald (PME) electrostatics under NPT (N, amount of substance; P, pressure; T, temperature) conditions. Receptor grid generation for the protein model and ligand preparation were processed by using previously described methodologies (47). The prepared ligand was subjected to the extraprecision (XP) mode of docking by using Glide v9.10.

Determination of total intracellular reduced thiol content. Late-log-phase cells were harvested, washed with a buffer (0.14 M Na_3PO_4, 0.14 M K_3PO_4, 0.14 M NaCl, and 3 mM KCl) (pH 7.4), and suspended in 0.6 ml of 25% trichloroacetic acid. After 10 min on ice, the denatured protein and cell debris were removed by centrifugation in a microcentrifuge for 10 min at 4°C. The thiol content of the supernatant solution was determined by using 0.6 mM 5,5′-dithio-bis(2-nitrobenzoic acid) (DTNB) (Ellman's reagent) in a buffer containing 0.2 M Na_3PO_4 (pH 8.0). The concentration of DTNB derivatives of thiols was estimated spectrophotometrically at 412 nm. Three replicates of each test were performed, and data are the means and standard deviations (SDs) from three observations.

Measurement of reactive oxygen species levels. Intracellular oxidant levels were determined by using H_2DCFDA dye (Sigma), which, when oxidized, becomes the highly fluorescent compound dichlorofluorescein (DCF) (49). Levels of ROS in promastigotes treated with H_2O_2 (4 h) or SAG and/or Amp B (8 h) were monitored by incubating aliquots of parasite cultures with 0.4 mM H_2DCFDA (optimal) for 15 min in the dark. The cells were washed with PBS (pH 7.2) and lysed with lysis buffer (1% SDS and 1% Triton X-100 in 10 mM Tris), and the fluorescence intensity of the supernatant was measured by using a spectrofluorimeter (LS55; PerkinElmer) with an excitation wavelength at 504 nm and an emission wavelength at 529 nm and expressed as relative fluorescence units (RFU). The reagent blank was prepared with 0.4 mM H_2DCFDA in lysis buffer (40). Each measurement was performed in triplicate, and data are expressed as means.

Cell viability assay. *Leishmania* promastigotes (1×10^6 cells/ml) were cultured in 24-well plates under elevated temperature and acidic pH (37°C and pH 5.5, respectively) for 48 h or exposed to H_2O_2 (4 h) or SAG and/or Amp B (8 h). Cells were harvested, and an MTT assay was performed according to

the manufacturer's protocol (In-VitroToxicology assay kit, MTT based; Sigma, USA). Briefly, 200 μl of the cell suspension was mixed with 20 μl of an MTT solution and incubated at 25°C for 3 h. To solubilize the resulting formazan crystals, 200 μl of MTT solubilization buffer was added, and the optical density of the solution was measured at 570 nm (40). The percent cell viability was determined by comparison with untreated *L. donovani* cultures. Each measurement was performed in triplicate, and data are expressed as the means for each set of replicates.

Determination of infection rates. For animal use, procedures used were reviewed and approved by the Animal Ethical Committee, Rajendra Memorial Research Institute of Medical Sciences (RMRIMS) (Indian Council of Medical Research [ICMR]). The RMRIMS (ICMR) follows the *Guide for the Care and Use of Laboratory Animals* (51). A total of 10^6 PEC macrophages were isolated from BALB/c mice after stimulation with 4% starch and plated onto glass coverslips in 3-cm dishes for 4 h at 37°C in the presence of a 5% CO_2 atmosphere. The nonadherent cells were removed by gentle washing with serum-free medium, and the adherent macrophages were incubated overnight in complete medium. To show the effect of GSK specifically on *Leishmania* PERK and other ways to null and void the effect of GSK on host PERK, promastigotes grown in regular medium for 4 days were pretreated with GSK2606414 for 3 h, washed with sterile PBS to remove the unreacted GSK (42, 48), harvested, and resuspended in PBS; the numbers of flagellated and nonflagellated forms were microscopically estimated; and the parasites were incubated with adherent macrophages at a multiplicity of infection of 10 in RPMI–10% FBS for 6 h at 37°C. Cells were washed three times in PBS to remove unattached parasites and again incubated for 24 h at 37°C in a CO_2 incubator. Coverslips were fixed by using methanol and stained with Giemsa stain according to standard protocols (50). The number of intracellular parasites was quantified by counting the total macrophages and the total intracellular parasites per microscopic field (100×, 1.3-numerical-aperture [NA] oil immersion objective with a BX41 microscope; Olympus), and the results were expressed as the number of intracellular parasites per 100 macrophages. At least 300 host cells, in triplicate, were analyzed.

Cloning and production of antibody against recombinant LdeIF2α protein. The LdeIF2α (GenBank accession number AY339369.1) open reading frame (ORF) was cloned into the pET-28a vector (Calbiochem) by using LdeIF2α forward primer 5′-TTTTGGATCCATGCGTGACCTGAACAAGCGCCA-3′ and LdeIF2α reverse primer 5′-TTTTAAGCTTGTCCGCATCCTCATCATCATCG-3′, containing the BamHI and HindIII restriction enzymes. The expressed recombinant protein was purified by Ni-nitrilotriacetic acid-agarose ion-exchange column chromatography according to the manufacturer's protocol (Qiagen). The homogeneity of the recombinant protein was checked by SDS-PAGE, and the protein was used to immunize mice for the generation of an antibody against recombinant LdeIF2α. Competent *Escherichia coli* DH5α and BL21(DE3) cells (Invitrogen) were used to maintain the plasmid constructs and for protein expression, respectively (data not shown).

Inhibition assay. GSK2606414 (Calbiochem), a PERK inhibitor, was added to promastigotes at a final concentration of 30 nM 1 h prior to treatment with elevated temperature and low pH or exposure to H_2O_2 and incubated for the indicated time periods. To study the infection rate, promastigotes were incubated with GSK2606414 for 3 h at 23°C in a BOD incubator prior to infection of mouse PECs. The parasites were subsequently washed with PBS (pH 7.2) three times and used for infection. The ROS scavenger NAC (Sigma-Aldrich) was added at a concentration of 5 mM before the promastigotes were subjected to H_2O_2 treatment. Thg, an ER stress generator, was added at a concentration of 1 μM (8, 12). BSO, an inhibitor of γ-Gcs, and DFMO, an inhibitor of Odc, were added at concentrations of 5 μM each (48). There were 3 replicates in each test, and the data are the means ± SDs of results from 3 experiments.

Statistical analysis. The data were statistically analyzed by using the Student *t* test and are presented as means and standard deviations of results for three determinations from at least two independent experiments. A *P* value of <0.05 was considered significant.

ACKNOWLEDGMENTS

The A2 antibody used in this study is a kind gift from Greg Matlashewski (McGill University, Canada). We are thankful to Geraldine Foster (Liverpool School of Tropical Medicine) for language editing of the manuscript.

This work has been funded by the Indian Council of Medical Research, Ministry of Health and Family Welfare, Government of India. K.A. is supported by a senior research fellowship from the Indian Council of Medical Research.

We declare that we have no conflict of interest. The funder has no role in study design, data collection and interpretation, or the decision to submit the work for publication.

REFERENCES

1. Saxena A, Lahav T, Holland N, Aggarwal G, Anupama A, Huang Y, Volpin H, Myler PJ, Zilberstein D. 2007. Analysis of the Leishmania donovani transcriptome reveals an ordered progression of transient and permanent changes in gene expression during differentiation. Mol Biochem Parasitol 152:53–65. https://doi.org/10.1016/j.molbiopara.2006.11.011.
2. McNicoll F, Drummelsmith J, Muller M, Madore E, Boilard N, Ouellette M, Papadopoulou B. 2006. A combined proteomic and transcriptomic approach to the study of stage differentiation in Leishmania infantum. Proteomics 6:3567–3581. https://doi.org/10.1002/pmic.200500853.
3. Clayton C, Shapira M. 2007. Post-transcriptional regulation of gene

expression in trypanosomes and leishmanias. Mol Biochem Parasitol 156:93–101. https://doi.org/10.1016/j.molbiopara.2007.07.007.
4. Haile S, Papadopoulou B. 2007. Developmental regulation of gene expression in trypanosomatid parasitic protozoa. Curr Opin Microbiol 10:569–577. https://doi.org/10.1016/j.mib.2007.10.001.
5. Dever TE. 2002. Gene-specific regulation by general translation factors. Cell 108:545–556. https://doi.org/10.1016/S0092-8674(02)00642-6.
6. Sonenberg N, Hinnebusch AG. 2009. Regulation of translation initiation in eukaryotes: mechanisms and biological targets. Cell 136:731–745. https://doi.org/10.1016/j.cell.2009.01.042.
7. Wek RC, Jiang HY, Anthony TG. 2006. Coping with stress: eIF2 kinases and translational control. Biochem Soc Trans 34:7–11. https://doi.org/10.1042/BST0340007.
8. Narasimhan J, Joyce BR, Naguleswaran A, Smith AT, Livingston MR, Dixon SE, Coppens I, Wek RC, Sullivan WJ, Jr. 2008. Translation regulation by eukaryotic initiation factor-2 kinases in the development of latent cysts in Toxoplasma gondii. J Biol Chem 283:16591–16601. https://doi.org/10.1074/jbc.M800681200.
9. Joyce BR, Queener SF, Wek RC, Sullivan WJ, Jr. 2010. Phosphorylation of eukaryotic initiation factor-2α promotes the extracellular survival of obligate intracellular parasite Toxoplasma gondii. Proc Natl Acad Sci U S A 107:17200–17205. https://doi.org/10.1073/pnas.1007610107.
10. Zhang M, Mishra S, Sakthivel R, Roja M, Ranjan R, Sullivan WJ, Jr. 2012. PK4, a eukaryotic initiation factor 2α (eIF2α) kinase, is essential for the development of the erythrocytic cycle of Plasmodium. Proc Natl Acad Sci U S A 109:3956–3961. https://doi.org/10.1073/pnas.1121567109.
11. Tonelli RR, Silva Da Augusto L, Castilho BA, Schenkman S. 2011. Protein synthesis attenuation by phosphorylation of eIF2a is required for the differentiation of Trypanosoma cruzi into infective forms. PLoS One 6:e27904. https://doi.org/10.1371/journal.pone.0027904.
12. Cloutier S, Laverdiere M, Chou M-N, Boilard N, Chow C, Papadopoulou B. 2012. Translational control through eIF2alpha phosphorylation during the Leishmania differentiation process. PLoS One 7:e35085. https://doi.org/10.1371/journal.pone.0035085.
13. Donnelly N, Gorman AM, Gupta S, Samali A. 2013. The eIF2α kinases: their structures and functions. Cell Mol Life Sci 70:3493–3511. https://doi.org/10.1007/s00018-012-1252-6.
14. Ward P, Equinet L, Packe J, Doerig C. 2004. Protein kinases of the human malaria parasite Plasmodium falciparum: the kinome of a divergent eukaryote. BMC Genomics 5:79. https://doi.org/10.1186/1471-2164-5-79.
15. Moraes MC, Jesus TCL, Hashimoto NN, Dey M, Schwartz KJ, Alves VS, Avila CC, Bangs JD, Dever TE, Schenkman S, Castilho BA. 2007. Novel membrane-bound eIF2alpha kinase in the flagellar pocket of Trypanosoma brucei. Eukaryot Cell 6:1979–1991. https://doi.org/10.1128/EC.00249-07.
16. Silva Da Augusto L, Moretti NS, Ramos TCP, Jesus TCL, Zhang M, Castilho BA, Schenkman S. 2015. A membrane-bound eIF2 alpha kinase located in endosomes is regulated by heme and controls differentiation and ROS levels in Trypanosoma cruzi. PLoS Pathog 11:e1004618. https://doi.org/10.1371/journal.ppat.1004618.
17. Gosline SJC, Nascimento M, McCall LI, Zilberstein D, Thomas DY, Matlashewski G, Hallett M. 2011. Intracellular eukaryotic parasites have a distinct unfolded protein response. PLoS One 6:e19118. https://doi.org/10.1371/journal.pone.0019118.
18. Chow C, Cloutier S, Dumas C, Chou MN, Papadopoulou B. 2011. Promastigote to amastigote differentiation of Leishmania is markedly delayed in the absence of PERK eIF2alpha kinase-dependent eIF2alpha phosphorylation. Cell Microbiol 13:1059–1077. https://doi.org/10.1111/j.1462-5822.2011.01602.x.
19. Tan S, Somia N, Maher P, Schubert D. 2001. Regulation of antioxidant metabolism by translation initiation factor 2α. J Cell Biol 152:997–1006. https://doi.org/10.1083/jcb.152.5.997.
20. Back SH, Scheuner D, Han JS, Song B, Ribick M, Wang J, Gildersleeve RD, Pennathur S, Kaufman RJ. 2009. Translation attenuation through eIF2α phosphorylation prevents oxidative stress and maintains the differentiated state in beta cells. Cell Metab 10:13–26. https://doi.org/10.1016/j.cmet.2009.06.002.
21. Rouschop KM, Dubois LJ, Keulers TG, van den Beucken T, Lambin P, Bussink J, van der Kogel AJ, Koritzinsky M, Wouters BG. 2013. PERK/eIF2α signaling protects therapy resistant hypoxic cells through induction of glutathione synthesis and protection against ROS. Proc Natl Acad Sci U S A 110:4622–4627. https://doi.org/10.1073/pnas.1210633110.
22. Moreno JA, Halliday M, Molloy C, Radford H, Verity N, Axten JM, Ortori CA, Wills AE, Fischer PM, Barrett DA, Mallucci DR. 2013. Oral treatment targeting the unfolded protein response prevents neurodegeneration and clinical disease in prion-infected mice. Sci Transl Med 5:206ra138. https://doi.org/10.1126/scitranslmed.3006767.
23. Gebauer F, Hentze MW. 2004. Molecular mechanisms of translational control. Nat Rev Mol Cell Biol 5:827–835. https://doi.org/10.1038/nrm1488.
24. Vonlaufen N, Kanzok SM, Wek RC, Sullivan WJ, Jr. 2008. Stress response pathways in protozoan parasites. Cell Microbiol 10:2387–2399. https://doi.org/10.1111/j.1462-5822.2008.01210.x.
25. Cohen-Freue G, Holzer TR, Forney JD, McMaster WR. 2007. Global gene expression in Leishmania. Int J Parasitol 37:1077–1086. https://doi.org/10.1016/j.ijpara.2007.04.011.
26. Rochette A, Raymond F, Corbeil J, Ouellette M, Papadopoulou B. 2009. Whole genome comparative RNA expression profiling of axenic and intracellular amastigote forms of Leishmania infantum. Mol Biochem Parasitol 165:32–47. https://doi.org/10.1016/j.molbiopara.2008.12.012.
27. Alcolea PJ, Alonso A, Gómez MJ, Sánchez-Gorostiaga A, Paz MM, González-Pastor E, Toraño A, Parro V, Larraga V. 2010. Temperature increase prevails over acidification in gene expression modulation of amastigote differentiation in Leishmania infantum. BMC Genomics 11:31. https://doi.org/10.1186/1471-2164-11-31.
28. Rosenzweig D, Smith D, Opperdoes F, Stern S, Olafson RW, Zilberstein D. 2008. Retooling Leishmania metabolism: from sand fly gut to human macrophage. FASEB J 22:590–602.
29. Debrabant A, Joshi MB, Pimenta PF, Dwyer DM. 2004. Generation of Leishmania donovani axenic amastigotes: their growth and biological characteristics. Int J Parasitol 34:205–217. https://doi.org/10.1016/j.ijpara.2003.10.011.
30. Wilson ME, Andersen KA, Britigan BE. 1994. Response of Leishmania chagasi promastigotes to oxidant stress. Infect Immun 62:5133–5141.
31. Van Assche T, Deschacht M, da Luz RAI, Maes L, Cos P. 2011. Leishmania-macrophage interactions: insights into the redox biology. Free Radic Biol Med 51:337–351. https://doi.org/10.1016/j.freeradbiomed.2011.05.011.
32. Channon JY, Roberts MB, Blackwell JM. 1984. A study of the differential respiratory burst activity elicited by promastigotes and amastigotes of Leishmania donovani in murine resident peritoneal macrophages. Immunology 53:345–355.
33. Alzate JF, Arias AA, Moreno-Mateos D, Alvarez-Barrientos A, Jiménez-Ruiz A. 2007. Mitochondrial superoxide mediates heat induced apoptotic like death in Leishmania infantum. Mol Biochem Parasitol 152:192–202. https://doi.org/10.1016/j.molbiopara.2007.01.006.
34. Mittra B, Cortez M, Haydock A, Ramasamy G, Myler PJ, Andrews NW. 2013. Iron uptake controls the generation of Leishmania infective forms through regulation of ROS levels. J Exp Med 210:401–416. https://doi.org/10.1084/jem.20121368.
35. Baird TD, Wek RC. 2012. Eukaryotic initiation factor 2 phosphorylation and translational control in metabolism. Adv Nutr 3:307–321. https://doi.org/10.3945/an.112.002113.
36. Raven JF, Koromilas AE. 2008. PERK and PKR: old kinases learn new tricks. Cell Cycle 7:1146–1150. https://doi.org/10.4161/cc.7.9.5811.
37. Singh KP, Zaidi A, Anwar S, Bimal S, Das P, Ali V. 2014. Reactive oxygen species regulates expression of iron-sulfur cluster assembly protein IscS of Leishmania donovani. Free Radic Biol Med 75:195–209. https://doi.org/10.1016/j.freeradbiomed.2014.07.017.
38. Charest H, Matlashewski G. 1994. Developmental gene expression in Leishmania donovani: differential cloning and analysis of an amastigote-stage-specific gene. Mol Cell Biol 14:2975–2984. https://doi.org/10.1128/MCB.14.5.2975.
39. Zhang W, Matlashewski G. 1997. Loss of virulence in Leishmania donovani deficient in an amastigote-specific protein, A2. Proc Natl Acad Sci U S A 94:8807–8811. https://doi.org/10.1073/pnas.94.16.8807.
40. Sardar AH, Kumar S, Kumar A, Purkait B, Das S, Sen A, Kumar M, Sinha KK, Singh D, Equbal A, Ali V, Das P. 2013. Proteome changes associated with Leishmania donovani promastigote adaptation to oxidative and nitrosative stresses. J Proteomics 81:185–199. https://doi.org/10.1016/j.jprot.2013.01.011.
41. Ghosh AK, Sardar AH, Mandal A, Saini S, Abhishek K, Kumar A, Purkait B, Singh R, Das S, Mukhopadhyay R, Roy S, Das P. 2015. Metabolic reconfiguration of the central glucose metabolism: a crucial strategy of Leishmania donovani for its survival during oxidative stress. FASEB J 29:2081–2098. https://doi.org/10.1096/fj.14-258624.
42. Kumar A, Das S, Purkait B, Sardar AH, Ghosh AK, Dikhit MR, Abhishek K, Das P. 2014. Ascorbate peroxidase, a key molecule regulating amphotericin B resistance in clinical isolates of Leishmania donovani. Antimi-

crob Agents Chemother 58:6172–6184. https://doi.org/10.1128/AAC.02834-14.
43. Goyard S, Segawa H, Gordon J, Showalter M, Duncan R, Turco SJ, Beverley SM. 2003. An *in vitro* system for developmental and genetic studies of Leishmania donovani phosphoglycans. Mol Biochem Parasitol 130:31–42. https://doi.org/10.1016/S0166-6851(03)00142-7.
44. Moreira W, Leprohon P, Ouellette M. 2011. Tolerance to drug-induced cell death favours the acquisition of multidrug resistance in Leishmania. Cell Death Dis 2:e201. https://doi.org/10.1038/cddis.2011.83.
45. Wiederstein M, Sippl MJ. 2007. ProSA-web: interactive Web service for the recognition of errors in three-dimensional structures of proteins. Nucleic Acids Res 35:W407–W410. https://doi.org/10.1093/nar/gkm290.
46. Kar RK, Ansari MY, Suryadevara P, Sahoo BR, Sahoo GC, Dikhit MR, Das P. 2013. Computational elucidation of structural basis for ligand binding with Leishmania donovani adenosine kinase. Biomed Res Int 2013:609289. https://doi.org/10.1155/2013/609289.
47. Kar RK, Suryadevara P, Sahoo BR, Sahoo GC, Dikhit MR, Das P. 2013. Exploring novel KDR inhibitors based on pharmaco-informatics methodology. SAR QSAR Environ Res 24:215–234. https://doi.org/10.1080/1062936X.2013.765912.
48. Purkait B, Kumar A, Nandi N, Sardar AH, Das S, Kumar S, Pandey K, Ravidas V, Kumar M, De T, Singh D, Das P. 2012. Mechanism of amphotericin B resistance in clinical isolates of Leishmania donovani. Antimicrob Agents Chemother 56:1031–1041. https://doi.org/10.1128/AAC.00030-11.
49. Oyama Y, Hayashi A, Ueha T, Maekawa K. 1994. Characterization of 2′,7′dichlorofluorescin fluorescence in dissociated mammalian brain neurons: estimation on intracellular content of hydrogen peroxide. Brain Res 635:113–117. https://doi.org/10.1016/0006-8993(94)91429-X.
50. Sen S, Roy K, Mukherjee S, Mukhopadhyay R, Roy S. 2011. Restoration of IFNγR subunit assembly, IFNγ signaling and parasite clearance in Leishmania donovani infected macrophages: role of membrane cholesterol. PLoS Pathog 7:e1002229. https://doi.org/10.1371/journal.ppat.1002229.
51. National Research Council. 2011. Guide for the care and use of laboratory animals, 8th ed. National Academies Press, Washington, DC.